

RESEARCH ARTICLE

10.1002/2015JB012650

Stochastic filtering for determining gravity variations for decade-long time series of GRACE gravity

Key Points:

- Statistically rigorous separation of signal and noise in a series of GRACE monthly gravity solution
- Destriping relies on covariance reflecting the spatiotemporal spectral features
- Allowing propagation of rigorous covariances for the destriped GRACE spherical harmonic coefficients

Correspondence to:

L. Wang,
leiwang@ldeo.columbia.edu

Citation:

Wang, L., J. L. Davis, E. M. Hill, and M. E. Tamisiea (2016), Stochastic filtering for determining gravity variations for decade-long time series of GRACE gravity, *J. Geophys. Res. Solid Earth*, 121, 2915–2931, doi:10.1002/2015JB012650.

Received 12 NOV 2015

Accepted 8 MAR 2016

Accepted article online 11 MAR 2016

Published online 8 APR 2016

Lei Wang^{1,2}, James L. Davis¹, Emma M. Hill³, and Mark E. Tamisiea⁴

¹Lamont-Doherty Earth Observatory, Columbia University, Palisades, NY, USA, ²Now at Department of Earth, Atmospheric and Planetary Sciences, Massachusetts Institute of Technology, Cambridge, Massachusetts, USA, ³Earth Observatory of Singapore, Nanyang Technological University, Singapore, ⁴National Oceanography Centre, Joseph Proudman Building, Liverpool, UK

Abstract We present a new stochastic filter technique for statistically rigorous separation of gravity signals and correlated “stripe” noises in a series of monthly gravitational spherical harmonic coefficients (SHCs) produced by the Gravity Recovery and Climate Experiment (GRACE) satellite mission. Unlike the standard destriping process that removes the stripe contamination empirically, the stochastic approach simultaneously estimates gravity signals and correlated noises relying on covariance information that reflects both the spatial spectral features and temporal correlations among them. A major benefit of the technique is that by estimating the stripe noise in a Bayesian framework, we are able to propagate statistically rigorous covariances for the destriped GRACE SHCs, i.e. incorporating the impact of the destriping on the SHC uncertainties. The Bayesian approach yields a natural resolution for the gravity signal that reflects the correlated stripe noise, and thus achieve a kind of spatial smoothing in and of itself. No spatial Gaussian smoothing is formally required although it might be useful for some circumstances. Using the stochastic filter, we process a decade-length series of GRACE monthly gravity solutions, and compare the results with GRACE Tellus data products that are processed using the “standard” destriping procedure. The results show that the stochastic filter is able to remove the correlated stripe noise to a remarkable degree even without an explicit smoothing step. The estimates from the stochastic filter for each destriped GRACE field are suitable for Bayesian integration of GRACE with other geodetic measurements and models, and the statistically rigorous estimation of the time-varying rates and seasonal cycles in GRACE time series.

1. Introduction

Monthly gravitational field solutions produced by the Gravity Recovery and Climate Experiment (GRACE) mission [Tapley *et al.*, 2004] have been used to infer mass changes on and below the surface of Earth, such as climate-driven water transport on land [Chen *et al.*, 2010; Landerer and Swenson, 2012; Wang *et al.*, 2013] and in the oceans [Boening *et al.*, 2011; Chambers and Schröter, 2011], ice mass balance of the cryosphere [Jacob *et al.*, 2012; Shepherd *et al.*, 2012; Harig and Simons, 2015], glacial isostatic adjustment (GIA) [Paulson *et al.*, 2007; Tamisiea *et al.*, 2007; Hill *et al.*, 2010] and crustal deformation due to great earthquakes [Han *et al.*, 2006; Heki and Matsuo, 2010; Wang *et al.*, 2012a, 2012b, 2012c].

The GRACE analysis centers provide monthly gravitational field solutions as spherical harmonic (Stokes) coefficients (SHCs), complete to a certain degree and order. Due to systematic instrument errors and imperfections in the background models (which remove the effects of solid earth tides, ocean tides, non-tidal atmosphere, oceanic variability, etc.), the GRACE-derived gravitational field SHCs, especially the short-wavelength (high-degree) Stokes coefficients, are contaminated by noise. Some of these errors manifest themselves as north-south elongated linear features (known as “stripes”) in the monthly global gravity maps. Many studies have therefore aimed at extracting “clean” geophysical signals from these raw GRACE SHCs. A degree-dependent isotropic Gaussian smoother [Jekeli, 1981; Wahr *et al.*, 1998] can effectively reduce the dominant short-wavelength errors, and has thus become a routine procedure in GRACE data post-processing. However, geophysical signals become apparent only if the smoothing radius of the Gaussian filter is large enough to smear out the stripe noise. Consequently, surface mass variations can be estimated only with a spatial resolution of several hundred km or even larger. The large smoothing radius prevents GRACE from resolving shorter-wavelength features in geophysical signals. In order to obtain better spatial resolution in

latitude, *Han et al.* [2005] constructed an order-dependent non-isotropic filter which yields an averaging function with an east-west elongated Gaussian profile. *Schrama et al.* [2007] developed an EOF (empirical orthogonal functions) approximation technique for the representation of signal and assessment of noise in the monthly GRACE solutions. *Davis et al.* [2008] designed a statistical filtering approach that uses a parameterized model describing the temporal evolution of the GRACE coefficients. *Zhang et al.* [2009] developed a low-pass non-isotropic filter to suppress noises in monthly GRACE gravity field.

Generally, two categories of GRACE processing approaches are commonly used in GRACE community. The first uses mascons, in which mass concentrations on Earth's surface are estimated directly from the intersatellite range-rate or acceleration [*Rowlands et al.*, 2010; *Sabaka et al.*, 2010; *Luthcke et al.*, 2013; *Watkins et al.*, 2015]. Regularizations can be applied directly in both spatial and temporal domains to stabilize the solution and suppress correlated stripe noise [*Rowlands et al.*, 2010], and hence no destriping is required.

The second approach uses the SHCs produced by GRACE data centers, and a destriping algorithm must be used. *Swenson and Wahr* [2006] (hereafter SW) demonstrated that the stripe noise are associated with correlations among errors in Stokes coefficients of even or odd parity at high orders. They empirically designed a moving window filter to reduce these correlations. [Certain technical details of the SW method can be found in *Duan et al.*, 2009.] Gaussian smoothing is required as an additional step, in order to diminish the influence of errors which are not removed by the moving window filter. This procedure successfully suppresses the stripe features in the map of GRACE-derived monthly surface mass anomalies and thus allows for a smaller Gaussian smoothing radius. Based on this basic idea, later studies [*Chambers*, 2006; *Chen et al.*, 2007; *Duan et al.*, 2009] built their own filters to study different geophysical phenomena.

Taking the GRACE Level-2 monthly Stokes coefficients as observations, regularization techniques have been introduced to improve the signal-to-noise ratio of the gravity estimates. For example, *Kusche* [2007] designed a non-isotropic smoothing kernel by using a prior signal covariance and approximate error covariance; *Swenson and Wahr* [2011] derived regularized solution by using the covariance matrix of the unconstrained GRACE solution. These regularization techniques successfully suppress the stripe noise without directly estimating the errors themselves.

Although the class of SW destriping/smoothing methods successfully reduce the appearance of stripe artifacts in GRACE solutions, no statistical information on the stripe noise per se is utilized in the procedure to discriminate signal from noise. It is therefore not possible to obtain statistically rigorous error estimates for the destriped GRACE SHCs using these techniques. This issue poses challenges for use of GRACE in stochastic models that estimate climate-related parameters [e.g., *Hill et al.*, 2010], since stochastic modeling approaches depend crucially on understanding the various signals and errors contained within the dynamic system, and the SW class of destriping methods do not preserve the necessary statistical information. In this study, therefore, we introduce a stochastic filter technique for statistically rigorous separation of geophysical signals and correlated "stripe" contamination in a series of GRACE monthly SHC estimates. The key to this procedure is to design covariance matrices for geophysical signals and the correlated error that reflect not only the spatial spectral features but also the temporal correlations among them. The realization of destriping purely relies on these statistical characterizations. A major benefit of the technique is that, with statistical information preserved, we are able to estimate the impact of the destriping on the SHC uncertainties. This approach would therefore be an appropriate "front end" for the statistically rigorous and self-consistent modeling of time-varying seasonal and longer-term signals, and statistical techniques recently developed to combine GRACE and other data for simultaneous estimation of GIA and present-day melting signals [*Hill et al.*, 2011].

The stochastic filter presented in this study is developed within a Bayesian framework that includes unknown "stripe" noise. It differs from the mascon solutions in that it processes the GRACE Level-2 SHCs solution rather than the Level-1 products such as the inter-satellite tracking data. Meanwhile, our method differs from the regularization methods [*Kusche*, 2007; *Swenson and Wahr*, 2011] in that it explicitly models and estimates the stripe noise in a Bayesian sense, and incorporates the temporal correlation in the estimation.

In this paper, we first present a theoretical description of the filter that includes the state vector, observation model, and dynamical (stochastic) model for the error and signal. We then describe the state covariance matrices that constrain the filter. Finally, we use the filter with the GRACE time series to assess its capabilities for destriping and signal estimation by comparison to analyses of GRACE data by the more traditional methods.

2. Description of the Stochastic Filter

We assume that the GRACE-derived SHCs at epoch t consist of the sum of the true gravity signal (which we will refer to as the “geophysical signal”), correlated stripe noise, and a zero-mean Gaussian-noise error:

$$y_{l,m}(t) = g_{l,m}(t) + \xi_{l,m}(t) + v_{l,m}(t) \quad (1)$$

where $y_{l,m}$ denotes the GRACE SHC for degree l and order m , $g_{l,m}$ is the time-varying geophysical signal relative to a static gravitational field, $\xi_{l,m}$ is the correlated stripe noise and $v_{l,m}$ is the Gaussian noise. Equation (1) is the observation equation for the stochastic filter, and can be written in matrix form as

$$\mathbf{Y}_t = \mathbf{A}_t \cdot \mathbf{X}_t + \mathbf{V}_t = \begin{bmatrix} \mathbf{I} & \mathbf{I} \end{bmatrix} \begin{bmatrix} \mathbf{X}_t^g \\ \mathbf{X}_t^\xi \end{bmatrix} + \mathbf{V}_t \quad (2)$$

where \mathbf{Y}_t is the observation vector of epoch t , \mathbf{X}_t is the time-variable state (parameter) vector, \mathbf{A}_t is the design matrix, and \mathbf{V}_t is the vector of zero-mean Gaussian noise with covariance \mathbf{R}_t . The superscripts g and ξ refer respectively to the geophysical signal and stripe noise, which together comprise the model state at epoch t . If the SHC data set consists of spherical harmonic degrees 2 to 60, then there are in total 7434 unknown parameters in the state \mathbf{X}_t , and the design matrix \mathbf{A}_t is a sparse matrix of dimension 3717×7434 .

To incorporate temporal variability, we will assume a simple linear system such that the state vector evolves as

$$\mathbf{X}_t = \mathbf{H}_t \cdot \mathbf{X}_{t-1} + \mathbf{W}_t \quad (3)$$

where \mathbf{H}_t is the state transition matrix, and \mathbf{W}_t is (stochastic) process noise. This model for temporal evolution is effectively similar to others in which the temporal evolution of the geophysical signal is constrained [e.g., *Kurtenbach et al.*, 2009; *Rowlands et al.*, 2010; *Sabaka et al.*, 2010; *Luthcke et al.*, 2013; *Watkins et al.*, 2015]. In the current implementation of the filter we assume that the geophysical part of the state evolves as a random walk, and that the stripe noise is uncorrelated from month to month, so that

$$\mathbf{H}_t = \begin{bmatrix} \mathbf{I} & \mathbf{0} \\ \mathbf{0} & \mathbf{0} \end{bmatrix} \quad (4)$$

The process noise \mathbf{W}_t , like the state vector, describes both the variability of the geophysical signal and the stripe noise:

$$\mathbf{W}_t = \begin{bmatrix} \mathbf{W}_t^g \\ \mathbf{W}_t^\xi \end{bmatrix} \quad (5)$$

We assume that \mathbf{W}_t is zero mean with covariance matrix \mathbf{Q}_t having structure

$$\mathbf{Q}_t = \begin{bmatrix} \mathbf{Q}_t^g & \mathbf{0} \\ \mathbf{0} & \mathbf{Q}_t^\xi \end{bmatrix} \quad (6)$$

That is, we assume that the stripe noise is uncorrelated with the temporal changes of the geophysical signal.

Under the assumptions we have made, we could in principle use a Kalman filter (including smoother) formulation to estimate the time-dependent state vector. One obvious challenge lies in the definition of the design matrix \mathbf{A}_t in equation (2). $\mathbf{A}_t^T \mathbf{R}_t^{-1} \mathbf{A}_t$ is in fact singular, a condition that leads to non-unique solutions for the state vector and an inability to separate the geophysical signal from the stripe noise. The impacts of this singularity can be avoided, however, by using information on the structure of expected correlations among the different parameters of the system that have quite different temporal evolutions. Thus, the structures of the covariance matrices \mathbf{R}_t and \mathbf{Q}_t have particular importance in our filter.

3. Stochastic Models and Covariance Matrices

We use a standard Kalman smoother formalism [e.g., *Ravishanker and Dey*, 2002] to estimate simultaneously the time-dependent geophysical and stripe signals. In any stochastic filter, the covariance matrices represent information that the filter uses to process the input signals and to estimate the time variable state. An appropriate choice for the covariance matrix removes many degrees of freedom from the problem. In this section, we describe the models and structure of the covariance matrices used in the current implementation of the stochastic filter.

3.1. Stochastic Stripe Model: Q_t^ξ

Swenson and Wahr [2006] found that the stripe noise is associated with the correlations among errors in SHCs. Their fundamental assumption is that SHC errors of different SH orders are uncorrelated, while correlations exist among the SHC errors of a given order that have degrees of equal parity (that is either even or odd). Specifically, at each epoch we can divide the SHCs of given order m into two sequences, Ξ_m^{even} and Ξ_m^{odd} , consisting of even and odd degrees, respectively. Here, given the order m , the even- and odd-degree sequences can be written as

$$\begin{aligned} \Xi_m^{\text{even}} &= \begin{cases} \{\xi_{m,m} & \xi_{m+2,m} & \xi_{m+4,m} & \cdots & \xi_{60,m}\}, & m \text{ even} \\ \{\xi_{m+1,m} & \xi_{m+3,m} & \xi_{m+5,m} & \cdots & \xi_{60,m}\}, & m \text{ odd} \end{cases} \\ \Xi_m^{\text{odd}} &= \begin{cases} \{\xi_{m+1,m} & \xi_{m+3,m} & \xi_{m+5,m} & \cdots & \xi_{59,m}\}, & m \text{ even} \\ \{\xi_{m,m} & \xi_{m+2,m} & \xi_{m+4,m} & \cdots & \xi_{59,m}\}, & m \text{ odd} \end{cases} \end{aligned} \quad (7)$$

The above sequences and stripe SHCs are implicitly indexed by the epoch t . We assume a maximum spherical harmonic degree of 60 since that is used in GRACE SHC files produced by Center for Space Research (CSR) at the University of Texas.

To approximate the stripe signal, Swenson and Wahr [2006] estimated coefficients for a series of quadratic polynomials for a moving window across similarly defined sequences of GRACE SHCs. Thus, for any given window, the stripe noise is assumed to vary smoothly and quadratically within the window and the geophysical signal is given by the residual SHC at the center degree of the window. The SW destriping/smoothing algorithm, although quite successful, is not easily implemented within the framework of a Bayesian filter, and, as we have discussed, it does not allow for estimation of post-destriped covariances.

The approach that we have taken in this study is to model the stripe noise at each epoch as a stochastic process indexed by position within the sequences defined by equation (7). The polynomial form of the SW approach would suggest an autoregressive model, the simplest of which is a random walk. Thus, we model each sequence using a random walk indexed by its position within the sequence. The submatrix consisting of the elements of the covariance matrix Q_t^ξ for each sequence above therefore has the form of a covariance matrix for a random walk [e.g., Williams, 2003, and references therein]. Additionally, we assume that the covariances of the stripe signal for SHCs in different sequences are zero.

We use a constant random-walk variance $(\sigma_m^{rw})^2$ for each coefficient in the sequence. Also, a non-zero variance $\sigma_{l_0,m}^2$ for the initial element in the sequence is required, since the stripe signal does not necessarily start at zero. Here, l_0 refers to the degree of the first element in the correlated noise sequence (7). Given order m , the value of l_0 is either m or $m + 1$ depending on the parity of m .

SW destriping filters usually does not avoid destriping at high degrees at low orders. However, in examining the root-mean-square (RMS) residuals after fitting secular, annual and semiannual terms to each of the raw SHCs, we observed that most of the coefficients of low orders, including those for high degrees, contain statistically significant annual and inter-annual geophysical signals. At low orders, no obvious correlations exist in the even and odd coefficient pairs. Taking the RMS residual as a measure of the magnitude of the stripe noise, we assume that the SHCs of order < 9 are free from stripe noise, even for those of high degrees. Consequently, the covariance matrix Q_t^ξ only contains information about stripe noise of order > 8 . Another feature we observe from above fitting is that the increase of the RMS residual is not continuous as the SH order increases; the order of magnitude of the RMS jumps around order 28 and also around order 40. In addition, the coefficients at the beginning of the sequences usually have larger variability than the other coefficients in the sequence (Figure 1). Thus, we increase the computed stripe noise variations by a factor of five for the first three coefficients in each sequence in order to take into account large systematic errors in (near-) sectoral coefficients. This choice is based on numerical experiments in which we analyze the statistics of the raw GRACE SHC series.

Referring to the magnitude of the RMS residual and experimenting with a number of choices, we selected to use the formulas listed in Table 1 to compute $\sigma_{l_0,m}^2$ and σ_m^{rw} of each order m . The values listed in Table 1 allow both $\sigma_{l_0,m}^2$ and $(\sigma_m^{rw})^2$ to increase with the spherical harmonic order m . These formulas are empirical and are based on our observation of the error characteristics in GRACE-measured SHCs. Figure 2 shows the computed prior variance of the stripe noises (diagonal component of Q_t^ξ) using the parameters given in Table 1. Table 1 and Figure 2 do not reflect the factor of five variance increase for the first three coefficients described above.

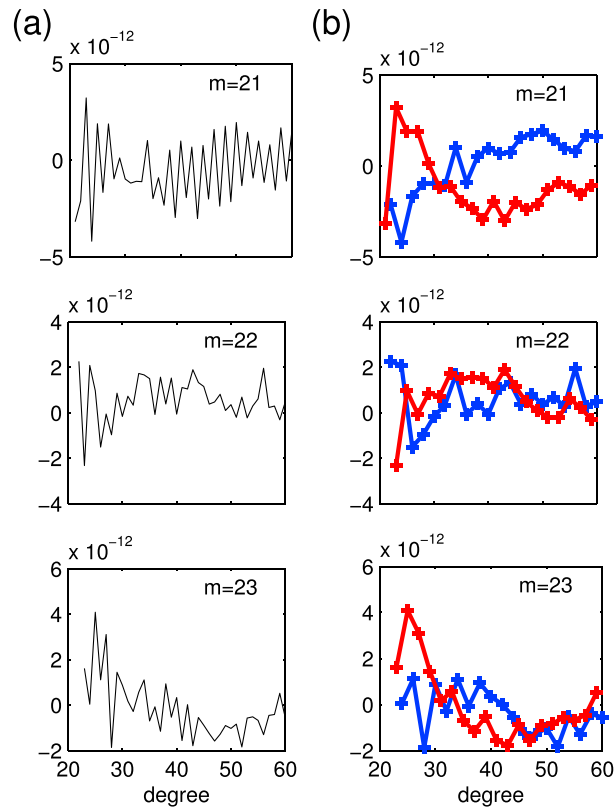


Figure 1. Stokes coefficients (C_{lm}) for orders $m = 21, 22$ and 23 (a) plotted for every degree and (b) plotted separately for even and odd degrees. The coefficients at the beginning of each of the odd and even sequences show large variations.

The above procedure yields approximate values for the statistical constraints of the stripe noise which are conservative in the sense that they are probably overestimates, since the prior modeling done in these initial tests is limited, and any unmodeled noise is interpreted as stripe noise. This approach is consistent with our principle of attempting to effectively separate stripe noise from geophysical signals while introducing as little overall constraint as possible into the filter. We therefore select larger noise variances (less constrained), rather than risk too-small (over-constrained) values, which can lead to biases.

3.2. Dynamic Gravity Model: Q_t^g

The covariance matrix Q_t^g contains information on the temporal evolution of geophysical signals that are detected by GRACE, including hydrological cycles, ocean mass variations, GIA, ice-mass changes and others [Tapley et al., 2004]. To obtain the prior statistics of mass changes, we analyze the available models and observations. First, we combine predictions from the GLDAS (Global Land Data Assimilation System) land water content model [Rodell et al., 2004] and the ECCO (Estimation of the Circulation and Climate of the Ocean) ocean bottom pressure model [Kim et al., 2007], together with a GIA model [Geruo et al., 2013] expressed in terms of secular mass change. In order to obtain prior information on the mass variation over Antarctica and Greenland, we integrate the GRACE-derived monthly mass variations over Greenland and Antarctica, as few models are available to completely account for the surface mass balance, dynamic ice loss and basal melting

Table 1. Parameters Used in the Stochastic Model for the GRACE Correlated “stripe” Noise^a

| m | $\sigma_{l_0,m}^2$ | $(\sigma_m^{rw})^2$ |
|---------------------|--|---------------------|
| $09 \leq m < 28$ | $10^{-24} + 10^{-22} \times (m - 9)$ | 10^{-22} |
| $28 \leq m < 40$ | $10^{-23} + 10^{-21} \times (m - 28)$ | 10^{-21} |
| $40 \leq m \leq 60$ | $10^{-22} + 3 \times 10^{-20} \times (m - 40)$ | 3×10^{-20} |

^aBoth $\sigma_{l_0,m}^2$ and $(\sigma_m^{rw})^2$ are unitless.

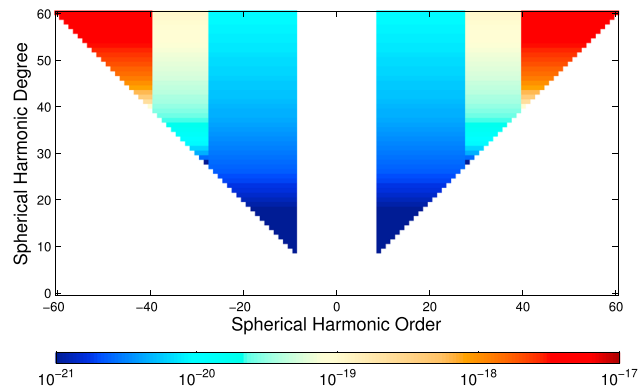


Figure 2. Prior variance (diagonal components of matrix Q_t^E) assigned to the dimensionless stripe noise. The variance increments by factor of 5 for the (near-) sectoral coefficients are not included.

that result in varying gravity field. We truncate the monthly mass variations predicted by the final combined model to degree 60 (Figure 3). Thus, we estimate the diagonal components of Q_t^g (i.e., variances of the SHCs representing variations in monthly global mass distribution) by calculating the degree variance of the model prediction [Pellinen, 1970; Rapp, 1973]

$$(\sigma_l^g)^2 = \frac{1}{2l+1} \sum_{m=0}^l (\Delta \bar{C}_{l,m}^2 + \Delta \bar{S}_{l,m}^2) \tag{8}$$

where $\Delta \bar{C}_{l,m}$ and $\Delta \bar{S}_{l,m}$ are the differences between the model-derived SHCs of any two consecutive months. At given degree l , we use the same value of $(\sigma_l^g)^2$ as the prior variance for the SHCs at all different orders m . Although a variety of signals still remain unmodeled, the combined model (GLDAS, ECCO, GIA and ice mass) estimates the dominant part of total mass redistribution variance.

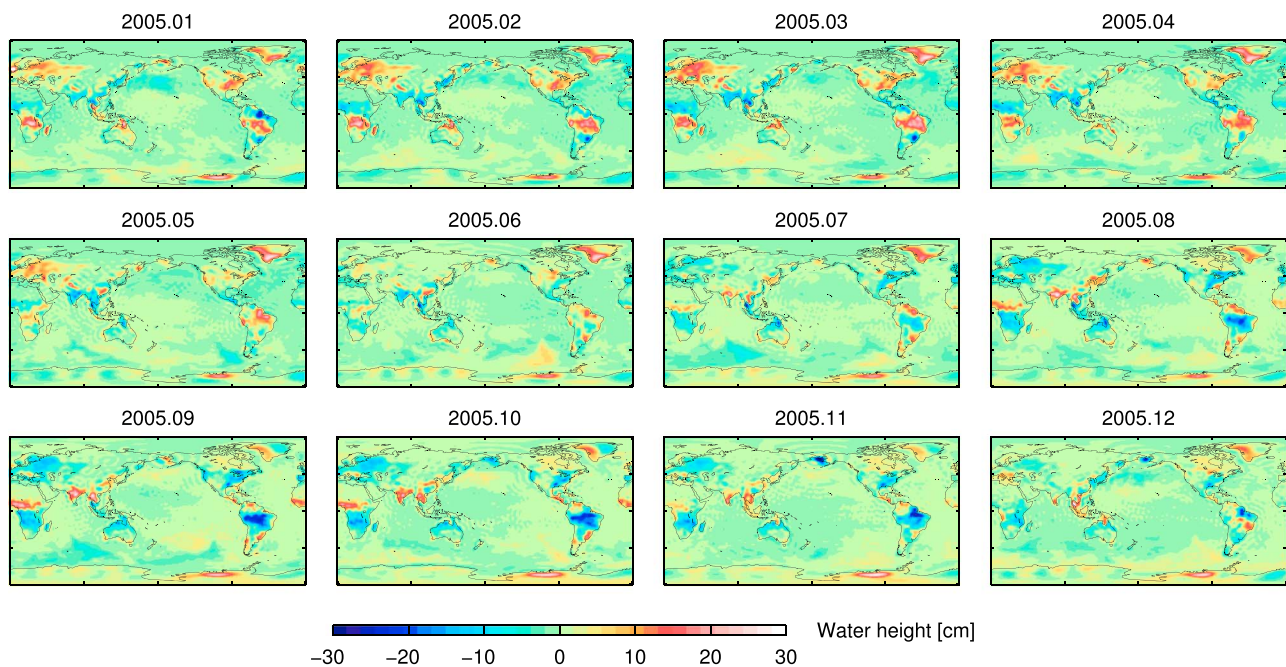


Figure 3. Global surface mass anomaly up to spherical harmonic degree 60, predicted by combining the GLDAS (Global Land Data Assimilation System) land water content model, the ECCO (Estimation of the Circulation and Climate of the Ocean) ocean bottom pressure model, the GIA model [Geruo *et al.*, 2013] and the mass variations over Greenland and Antarctica derived by GRACE. Mass anomalies are presented in terms of equivalent water thickness [Wahr *et al.*, 1998].

We also make the assumption that the SHCs are uncorrelated with each other, so the matrix Q_t^g is diagonal. This assumption does not reflect the spatial correlation of signals, and we will incorporate constraints for spatial correlations in a future study.

To examine the sensitivity of the stochastic filter to changes in the *a priori* matrix Q_t^g , we perform analyses with modified values. When we decreased the *a priori* covariance of mass variation by factor of 4, we found an RMS difference of 8.4 mm (i.e., an 18% change) in mass estimate, and 5 mm (5%) in the 1- σ uncertainty estimate. If we increase the covariance by factor of 4 instead, the RMS difference is 7.9 mm (17%) in mass estimate and 14.3 mm (16%) in the uncertainty estimate. Thus, it is not necessary to have a highly accurate model for Q_t^g that includes all small-scale contributions to the *a priori* covariance, such as those associated with the high mountain glaciers, inland seas and great earthquakes.

3.3. Observational Error Model: R_t

The formal errors for the monthly gravity SHCs generated by the GRACE data center are a reasonable choice to describe the observational white noise associated with estimated SHCs, since they are based on propagation of the “noise-only” covariances [Tapley *et al.*, 2005]. We use the GRACE RL05 full formal error covariance, provided by CSR, to build R_t for all RL05 monthly solutions.

Because only the diagonal components of the formal error covariance matrix are publicly accessible to GRACE Level-2 data users, and the full covariance matrices require a large amount of memory (105 Mb each and 12G for a decade) and increase computation time, we also test the feasibility of building a simplified diagonal matrix R_t by using these publicly available diagonal components. Based on tests we performed, using a diagonal R_t instead of the full covariance matrix does not alter the results significantly. Use of diagonal R_t does, however, dramatically expedite the computation by avoiding the inversion of a full matrix. Therefore, in practice, it is justified to only use a diagonal matrix R_t to describe the observational white noise when the stochastic filter is applied.

As mentioned in section 3.1, observational white noise is assumed to be the only error source for the Stokes coefficients with $m < 9$. By fitting and removing constant, annual, semi-annual and secular terms from the 118 monthly values of Stokes coefficients with $m < 9$, we found the GRACE formal errors of these coefficients likely underestimate the actual error if we assume the residuals are due entirely to observational errors. Thus, we used the RMS residuals to calculate the variance of observational white noise in these coefficients. This procedure likely overestimates the errors since mass variabilities on temporal scales other than purely annual and semi-annual exist [Davis *et al.*, 2012].

4. Results

In this section, we apply the stochastic filter to GRACE RL05 Level-2 monthly gravitational field solutions produced by CSR at the University of Texas [Bettadpur and the CSR Level-2 Team, 2012]. The reference field subtracted from the GRACE monthly solutions in our stochastic filter processing is the GRACE GGM03S (up to degree 60), which is based on the analysis of four years of GRACE in-flight data between January 2003 and December 2006. The results are then compared with those estimated by using the destriping and smoothing procedures described by SW.

4.1. Global Monthly Solutions

Figure 4 shows the estimated geophysical signal (surface mass) by applying the stochastic filter to GRACE RL05 solutions, while Figure 5 shows estimated stripe noise. As is common, we express the change in terms of equivalent water height [Wahr *et al.*, 1998] throughout this article despite the fact that GRACE-derived gravitational changes contain additional signals such as GIA and earthquake deformations. To compare with the GRACE Tellus solutions under the same time reference (see below), the mass anomalies shown in Figure 4 are relative to the mean of the twelve monthly solutions in 2004. The estimates in Figure 4 have not been spatially smoothed by convolution with a Gaussian filter, although suppression of high-degree signal seems to be innate to the filter design. Examination of Figure 4 reveals that the stochastic filter successfully removes most of the north-south stripes from the raw GRACE fields, and successfully preserves true geophysical signals, even without applying the Gaussian spatial smoothing. Seasonal mass variations associated with the hydrological cycle are observed in regions such as the Amazon Basin, the Congo Basin, South Asia, and Northern Australia. In addition, the secular trends in mass changes are apparent over the regions of Antarctica, Greenland and Alaska that are experiencing long-term ice mass loss.

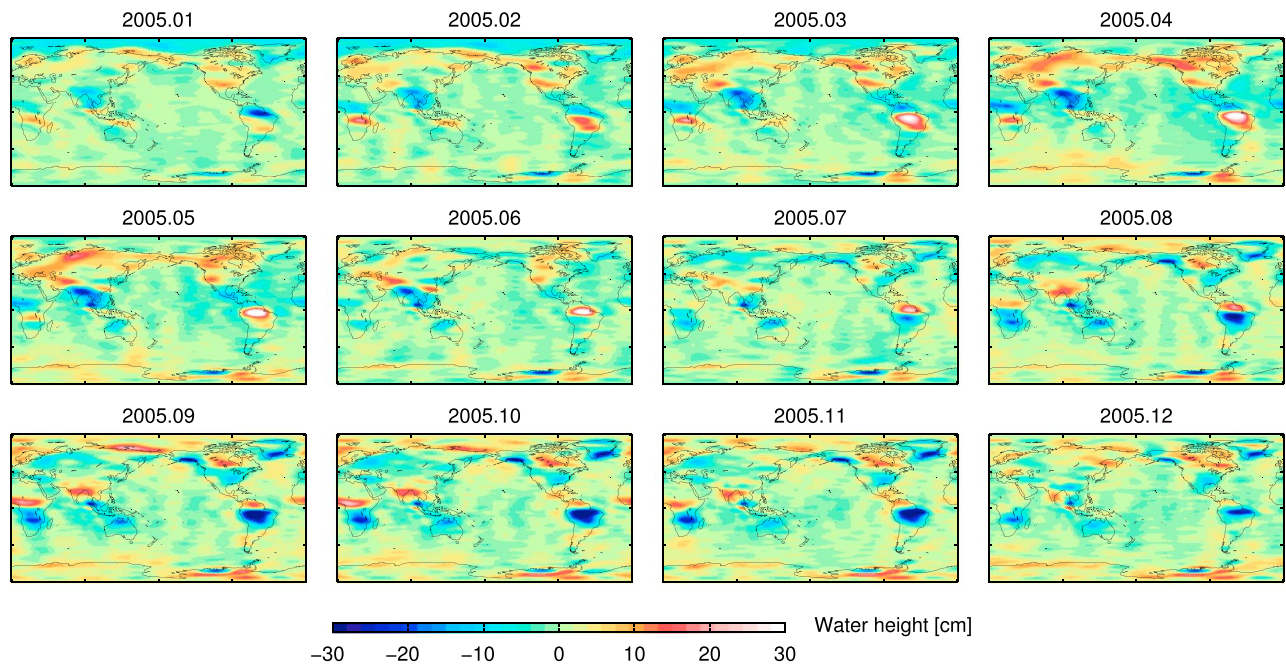


Figure 4. Monthly surface mass anomalies for 2005 from the stochastic filter, using GRACE RL05 Level-2 monthly gravitational fields produced by CSR. No spatial smoothing has been applied.

For comparison with the SW method, we downloaded GRACE-estimated monthly mass changes from the JPL GRACE Tellus website (<http://grace.jpl.nasa.gov/data/gracemonthlymassgridsoverview/>). These monthly mass changes are estimated by applying the destriping method described in *Swenson and Wahr [2006]* to CSR RL05 monthly GRACE data. Over land, a 300 km-wide Gaussian filter has been applied to the data after destriping, and a GIA correction has been applied. Over the oceans, a Gaussian filter with a half-width of 500 km has been applied, and the data are truncated at spherical harmonic degree 40. In addition, a leakage correction procedure has been applied in order to reduce the land signal leakage onto ocean signal. The mass anomaly

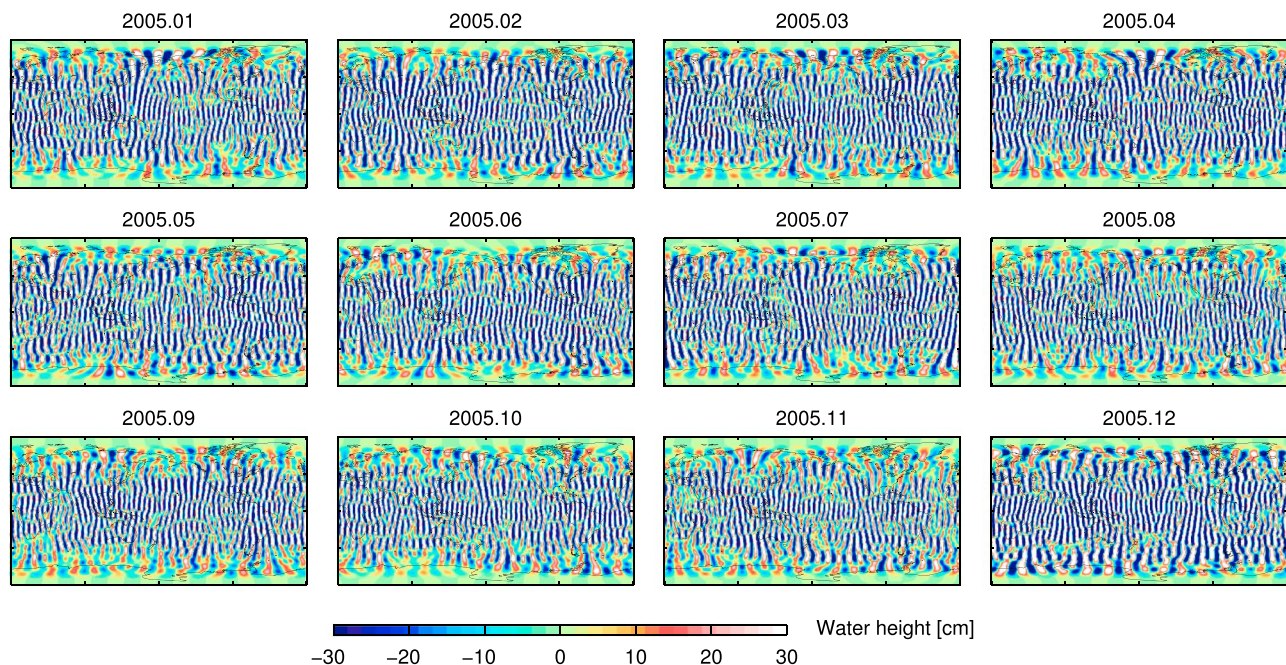


Figure 5. Monthly stripe noise estimates for 2005 from the stochastic filter, using GRACE RL05 Level-2 monthly gravitational fields produced by CSR.

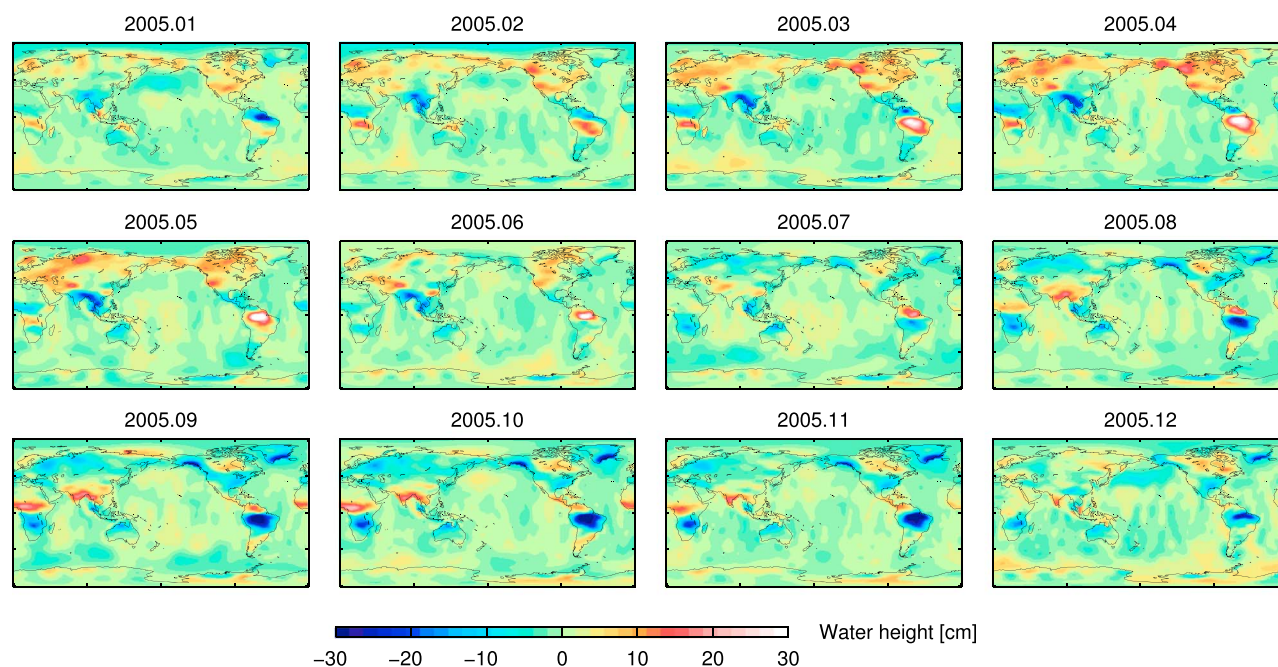


Figure 6. Monthly surface mass anomalies for 2005 from GRACE Tellus website (<http://grace.jpl.nasa.gov>). The monthly GRACE fields are processed based on the SW destriping procedure described in Swenson and Wahr [2006], followed by spatial smoothing using a 300 km wide Gaussian filter over land, and a 500 km wide Gaussian filter as well as the truncation up to degree 40 over ocean. Leakage correction has been applied to suppress the leakage of land signals into oceans. The GIA signals, which were removed in the GRACE Tellus processing, have been added back.

over ocean is relative to the time average from January 2005 to December 2010, while the mass anomaly over land is relative to the mean over January 2004 to December 2009. Therefore, we first unify the reference field for both land and ocean so that the GRACE Tellus mass anomalies are relative to the global mean of 2004. In order to compare with our stochastic filter result, we add the GIA corrections that have been applied to both land and ocean back to the GRACE Tellus monthly mass-change estimates [Geruo *et al.*, 2013]. Figure 6 shows the GRACE Tellus solutions (with the GIA model added back) for 2005. By comparing Figures 4 and 6, we can see that the stochastic approach and the SW destriping/smoothing technique both diminish the systematic stripe noise from the monthly fields, and yield mass-change estimates consistent with those predicted by combining GLDAS, ECCO, and GIA models (Figure 3). The difference between estimates from our stochastic filter and the GRACE Tellus solution could result from the errors in either or both sets of solutions, and also from the Gaussian smoothing, spherical harmonic truncation and the leakage correction that have been applied during the GRACE Tellus processing. Despite these issues, we compare to the GRACE Tellus solutions because they provide estimates independent of our analysis.

Remanent stripe features can be seen in the results from both methods. In the stochastic filter technique we assume the stripe noises are temporally independent, and only the gravity signals are correlated in time. Remanent stripe features in the mass changes estimated using the stochastic filter (Figure 4) indicate that temporal correlations may also exist among stripe features. An obvious characteristic in Figure 6 is that more remanent north-south stripe features exist over the equatorial region than at mid and high latitudes. The SW destriping procedures fit a polynomial to a sequence of coefficients of a given spherical harmonic order, and remove the fitted polynomial from the original coefficients. However, as can be seen in Figure 1, the sectoral and near-sectoral coefficients (i.e., the several coefficients at the beginning of the coefficient sequence to be fitted) generally carry large errors. These errors cannot be effectively modeled by a polynomial due to their large variations. Consequently, relatively large errors still remain in these (near-)sectoral coefficients after destriping, leading to noisier equatorial estimates. By allowing larger variance for the stripe noises in these coefficients (as discussed in section 3.1), our stochastic filter takes into account these (near-)sectoral errors.

Compared to the GRACE Tellus solutions in Figure 6, the monthly mass changes derived by our stochastic filter (Figure 4) show more small-scale features, or larger high-frequency components that could reflect either signal or noise (or both). Several known factors could contribute to these features: First, no spatial smoothing filter of

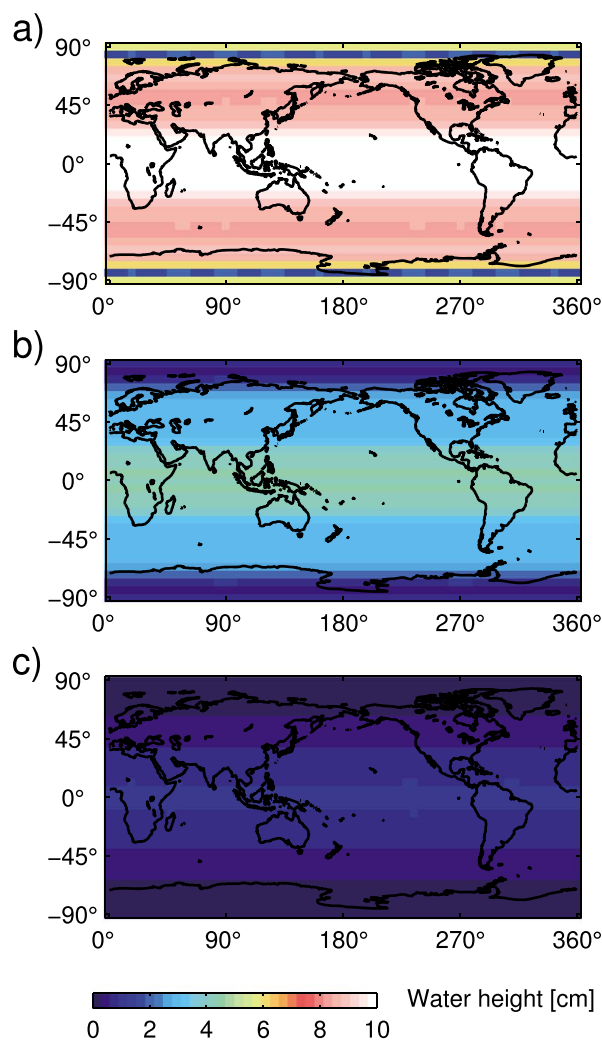


Figure 7. (a) Uncertainty ($1-\sigma$) of the surface mass anomaly for May 2005 from the stochastic filter. No spatial Gaussian smoothing has been applied. (b) Estimated uncertainty after applying Gaussian smoothing of width 300 km. (c) Same as (b), except a smoothing width of 750 km.

any type has been applied in the stochastic filter, while the Gaussian filter and spherical harmonic truncation have been applied in the SW destriping/smoothing procedure; Second, in the dynamic gravity model for the stochastic filter, we used the temporal correlations in the gravity signal but have not, in this study, taken into account the obvious spatial correlation.

A distinctive advantage of the new technique in this study is that we are able to estimate uncertainties for the surface mass estimated by GRACE using a Bayesian framework. Figure 7a shows estimated uncertainties for the mass anomalies in Figure 4 derived by our stochastic filter. Here, we show the uncertainty estimate in May 2005 as an example. It is clear that the estimated uncertainties increase toward the equator. The solution in May 2005 has a minimum uncertainty of 1.7 cm around the poles and a maximum uncertainty of ~ 10.5 cm around the equator. The ability to estimate uncertainties for the solutions is a notable advantage of using this Bayesian technique. Care must be taken in interpreting the error field of Figure 7a, however, since the degree of spatial coherence (correlation) of the errors cannot be discerned from visual inspection of the plot. Detailed discussion of the error correlations can be found in section 4.4.

Errors in GRACE-estimated mass change depend on latitude and smoothing radius [Wahr *et al.*, 2006]. Although the uncertainty estimates shown in Figure 7a may at first appear too large compared to those of Wahr *et al.* [2006] (for example), they are associated with our destriped field that has had no Gaussian smoothing applied. The uncertainties shown in Figure 7a allow the statistically rigorous error propagation in the

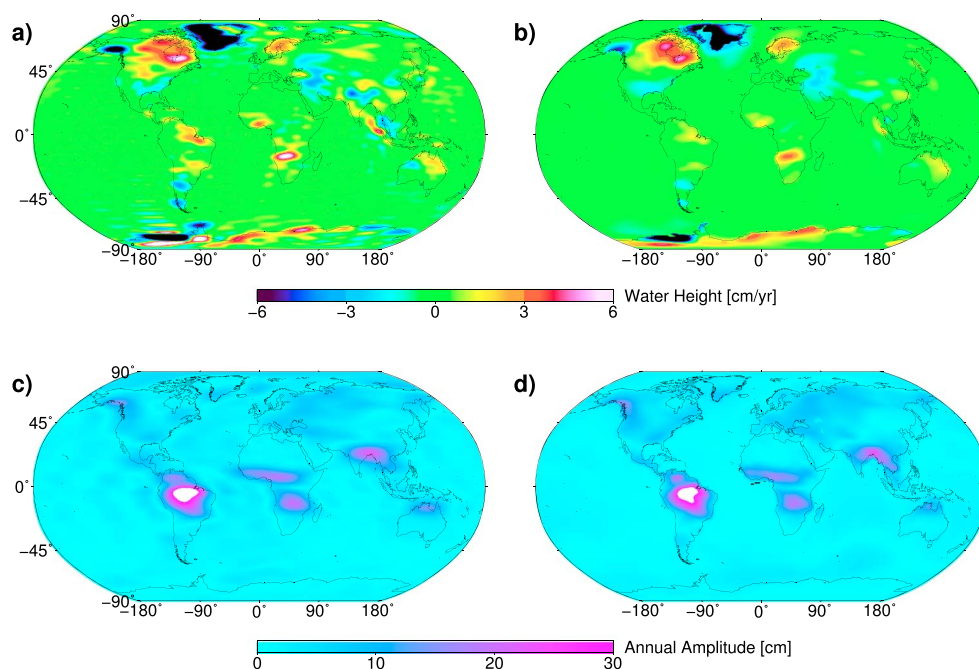


Figure 8. The secular trend (a and b) and annual amplitude (c and d) fitted from the stochastic filter estimate (a and c) and the GRACE Tellus solution (b and d). The period for the least square fitting spans from July 2003 to April 2013.

further computations of Gaussian smoothing or regional averages. Figures 7b and 7c show the estimated uncertainties when we apply the 300 km and 750 km Gaussian smoothing to the stochastic filter estimates, respectively. The uncertainty magnitudes vary from ~ 0.5 cm around the poles to ~ 4.4 cm over the equator in the case of 300 km Gaussian smoothing (Figure 7b), and from ~ 0.2 cm to ~ 1.0 cm in the case of 750 km Gaussian smoothing (Figure 7c). By analyzing the earlier release of GRACE gravity field solutions consisting of SHCs up to degree and order 120, *Wahr et al.* [2006] conclude that, for 750 km Gaussian smoothing, the uncertainties in the GRACE mass estimates (averaged over 22 months) vary from ~ 0.8 cm near poles to ~ 2.8 cm near equator. Thus, when the fields are smoothed, the uncertainty estimates from our stochastic filter are more consistent with those of *Wahr et al.* [2006], although the stochastic filter estimates are smaller.

Over the oceans, the stochastic filter estimates more small-scale features than the SW-plus-smoothing method. The smoother estimate over the oceans in the GRACE Tellus solutions are attributable to the spherical harmonic truncation up to degree 40, the Gaussian smoothing (radius of 500 km) and the leakage correction that have been applied to estimate the ocean signals. The 500km wide Gaussian smoothing is selected by the GRACE Tellus processing because it yields the best fit to the combination of altimetry and Argo data [*Chambers and Bonin*, 2012]. Because in current study we implement the stochastic filter in the spherical harmonic domain, the high-frequency signals over the oceans reflect the inevitable correlation between ocean and land in the spherical harmonic representation, and the globally consistent spatial resolution produced by our current stochastic filter. Therefore, further Gaussian smoothing might be useful if mass variations over oceans are studied. When the stochastic-filtered estimates are used for specific studies, the statistically rigorous estimate of the uncertainty, as shown in Figure 7, is important for estimating the mass variation. It allows the rigorous evaluation of the destriping impact on the GRACE estimate, and therefore proper weighting of the GRACE data for the specific application.

4.2. Secular Trend and Annual Amplitude

In Figure 8 we compare interannual signals and annual amplitudes for the stochastic filter and GRACE Tellus estimates. Both solutions show significant secular trends (Figures 8a and 8b) over regions such as Hudson Bay and Fennoscandia (which are associated with GIA), and over areas like Greenland, Antarctica, Alaska and Patagonia (reflecting mainly ice mass variations). Figures 8c and 8d also show similar annual amplitudes resulting from periodic terrestrial water storage variations over the Amazon Basin, Congo Basin, Southeast Asia, Northern Australia, Siberian Plain, and Canadian Coastal Mountains areas.

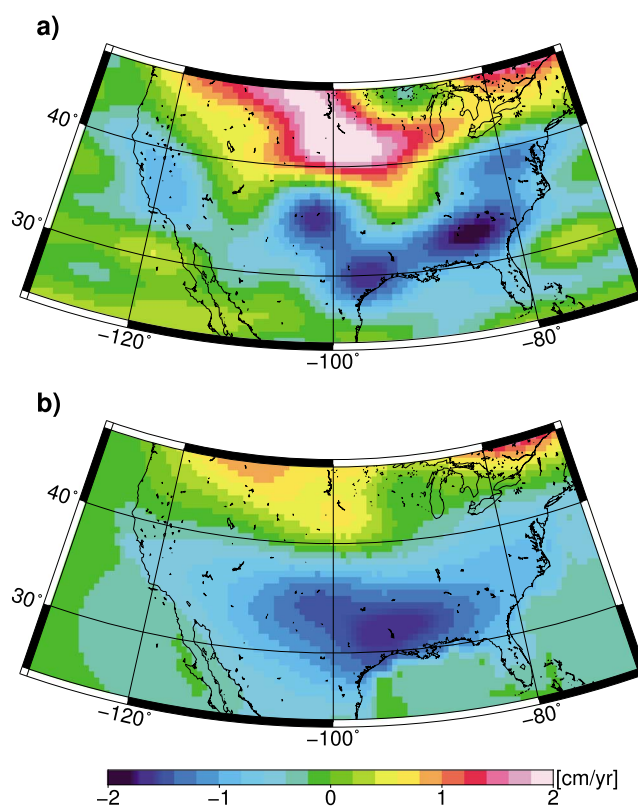


Figure 9. The secular trend in the terrestrial water storage variations over the United State derived from (a) the stochastic filter and (b) GRACE Tellus solution by fitting the estimates from July 2003 to April 2013.

Secular trends fitted from the stochastic filter estimates (Figure 8a) are of greater magnitudes than the trend values in the GRACE Tellus solution (Figure 8b). The SW destriping and smoothing procedures adopted by the GRACE Tellus processing cause mass signal attenuation at small spatial scales [Landerer and Swenson, 2012]. Although GRACE Tellus provides gridded scaling factors over land to restore the mass signal attenuation, these scaling factors are not suitable for restoring long-term trend signals, because they are derived by applying the same SW destriping/smoothing to a terrestrial hydrology model, which is subject to substantial uncertainty in the secular trend [Landerer and Swenson, 2012]. The effect of signal attenuation is illustrated by Figure 9, which compares the trends in the terrestrial water storage variation over the United States derived from the stochastic filter and GRACE Tellus. Although both techniques are inevitably subject to signal attenuation, the stochastic filter (Figure 9a) effectively localizes the draught signals in California and Texas [Watkins *et al.*, 2015], while these draught-induced features are smeared together over a broader area in the GRACE Tellus results (Figure 9b). The secular signals over this region as estimated by the stochastic filter (Figure 9a) share many of the same features with the JPL RL05M mascon solution in both spatial pattern and magnitude [see Figure 13 in Watkins *et al.*, 2015], although they are not exactly the same. Lower spatial resolution leads to smaller magnitudes in the secular trend. This would explain why the stochastic filter estimates larger secular trend than that from the GRACE Tellus as shown in Figure 8. More examples can be found in section 4.4.

Over oceans, the stochastic filter (Figure 8c) estimates noisier annual amplitudes than the GRACE Tellus solution (Figure 8d). It should be due to the truncation (above SH degree of 40) and the 500 km Gaussian smoothing applied in the GRACE Tellus solution. An obvious feature in the secular trend estimate by the stochastic filter (Figure 8a) is the east-west “stripes” in the oceans, such as over the west coast of Antarctica, the western Pacific Ocean, and the southern Indian Ocean. This suggests that the stripe noise model in the stochastic filter may not completely model the systematic errors in the GRACE monthly gravity solution. Also, it would indicate the existence of temporal correlations in the GRACE systematic error, because these horizontal “stripes” show up in the secular trend estimate. We leave to future study this issue of temporal correlated systematic error.

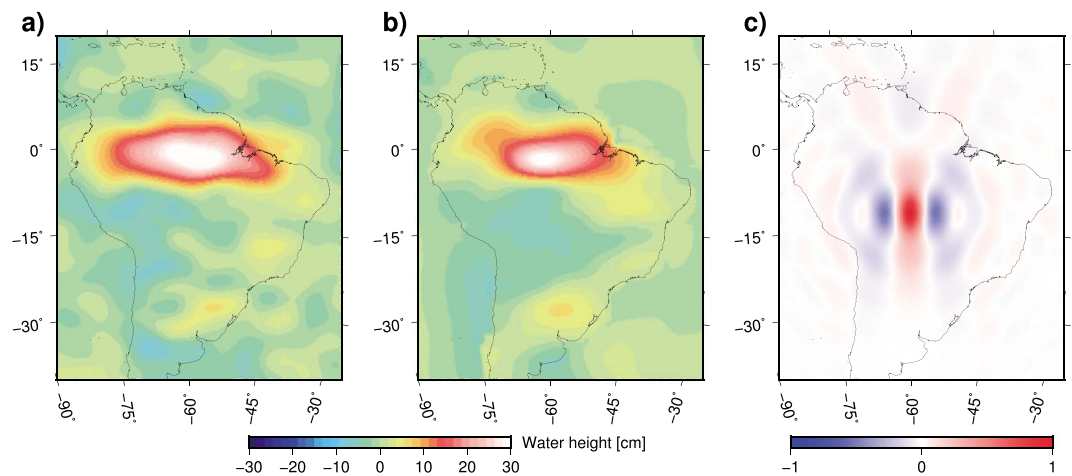


Figure 10. Comparison of the mass changes over the Amazon basin for June 2005 estimated by (a) the stochastic filter and (b) GRACE Tellus data (SW destriping). (c) The correlation coefficients of mass estimates between a location in the middle of Amazon basin (60.4°W , 12°S) and its surrounding locations, estimated by the stochastic filter.

4.3. Single-Month Comparison

For a more detailed comparison of the spatial resolution of these two destriping techniques, we examine the estimated mass changes over the Amazon Basin for a single month (June 2005). As the least-squares fitting for secular trends and seasonal amplitudes acts as an additional low-pass filter, this “single-month” comparison better reflects the destriping effectiveness of the stochastic filter. Figures 10a and 10b show the mass changes for June 2005 over the Amazon basin estimated by the different approaches. Both the stochastic filter (Figure 10a) and the SW destriping/smoothing (Figure 10b) estimate significant positive mass anomalies in the northern basin, and negative signals in the south. The primary discrepancies are over the surrounding oceans, where the result of the SW method (Figure 10b) shows less spatial variations. This difference for the oceans should result from the aforementioned smoothing/truncation processes and leakage correction applied in the GRACE Tellus solutions. No Gaussian smoothing has been applied to the estimate from the stochastic filter (Figure 10a).

As previously mentioned, one of the major advantages of the stochastic filter destriping technique is that it estimates statistically rigorous covariance, which enables the evaluation of the impact of destriping on the mass estimations using GRACE. Although the error fields of the mass estimates are shown in Figure 7, another piece of critical error information conveyed by the estimated covariance, namely the spatial correlation of the errors, cannot be discerned from those plots. The computation of the destriping-induced spatial correlation among mass estimates uses the design matrix that transforms the coefficients in the SH domain to the spatial values on a global grid. Figure 10c shows error correlations in the estimated mass between a location in the middle of the Amazon basin (60.4°W , 12°S) and its surrounding locations. This result is important since it reveals the statistical consequence of the destriping for the first time. It demonstrates that the destriping procedure actually results in positive correlations in the south-north direction and negative correlation in the west-east direction of the estimated mass anomalies. The full error covariance (correlation) matrix estimated by the stochastic filter, therefore, enables the statistically rigorous estimation of the average mass variation at basin scales, which will be discussed in the following section.

4.4. Average Mass Estimate at Basin Scales

Here, we compare the average mass changes of basin scales estimated by the stochastic filter with the GRACE Tellus solution and the mascon solution. In the results of the stochastic filter, the full spatial correlations, as discussed in section 4.3, have been used when the basin averages are computed. This is different from many previous studies that ignore the statistical impact of destriping on the mass estimation, and simply calculate the arithmetic average of the estimates within the basins.

Figure 11 compares the average mass estimates at various spatial scales ranging from $\sim 100,000\text{ km}^2$ (Alaska glaciers) to $\sim 2,000,000\text{ km}^2$ (Greenland), for the stochastic filter, the GRACE Tellus solution (over unglaciated regions) and the mascon solution [Luthcke et al., 2013] (over glaciated regions). Figure 11a–h are ordered by increasing area. Here, the full error covariance matrices have been taken into account when the basin averages are computed from the stochastic filter solution. As shown in Figure 11, the larger the spatial scale for

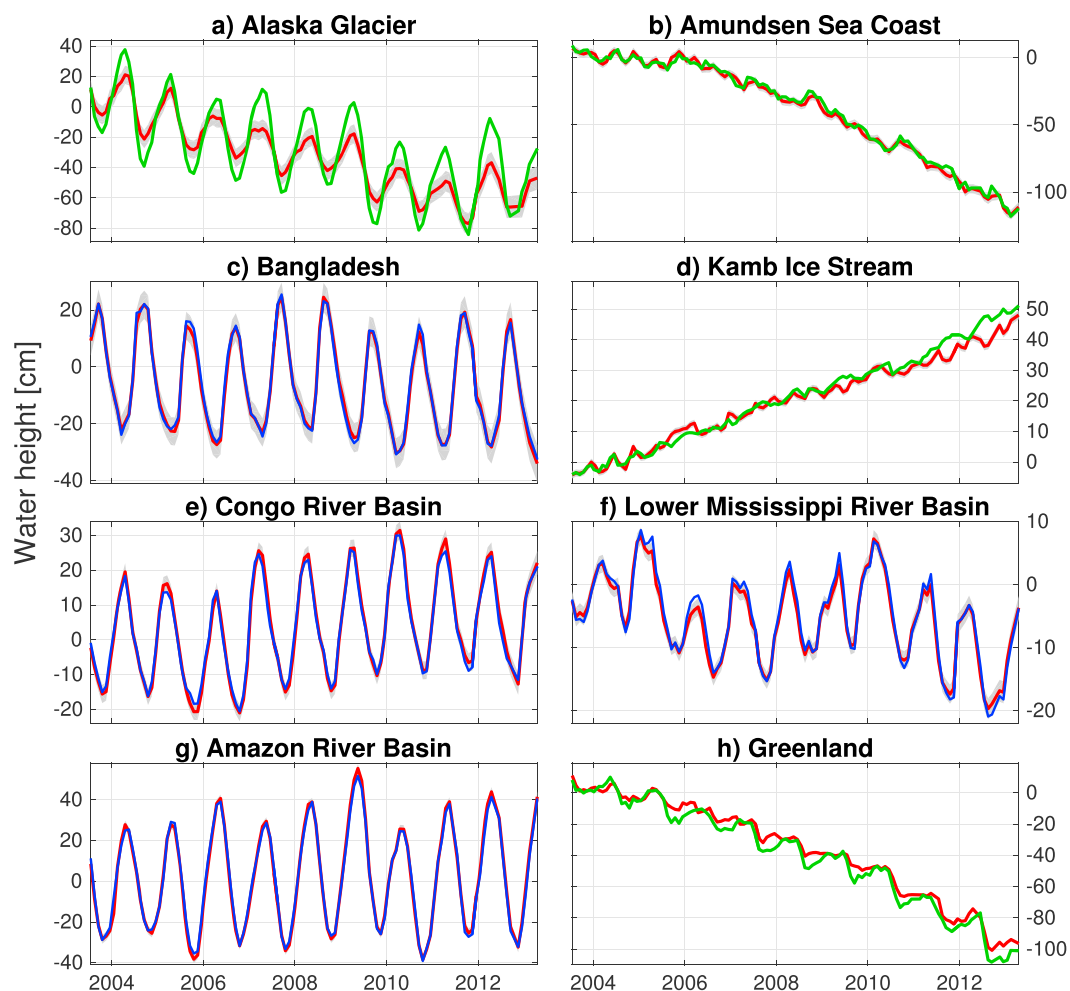


Figure 11. Comparisons of the average mass variations over different basins estimated by the stochastic filter (in red), the GRACE Tellus solution (in blue) and the mascon solution (v16) [Luthcke *et al.*, 2013] (in green). The shaded grey areas indicate the uncertainty estimates from the stochastic filter. The plots from (a) to (h) are ordered by increasing area, and their scales are different.

averaging, the smaller the uncertainty magnitude estimated by the stochastic filter. For example, the estimated uncertainty is ~ 6 cm for the average mass variation over the Alaska glaciers, compared with the value of ~ 1 cm over Greenland. (The scales of the plots are different.) Over major river basins such as the Bangladesh, Congo, Amazon and lower Mississippi river basins (Figures 11c, 11e, 11g and 11f), both solutions (the stochastic filter solution and the GRACE Tellus solution) show fairly consistent seasonal variations. The discrepancies between the two solutions are mostly within the uncertainty range derived by the stochastic filter, which would validate the error models assigned to the stochastic filter.

Over the areas experiencing long-term ice mass loss/gain which GRACE Tellus data are not suitable to study, we compare the stochastic filter estimate with the mascon solution [Luthcke *et al.*, 2013]. Although the comparisons are made for a wide range of spatial scales, such as over the Alaska glaciers, the Amundsen sea coast, the Kamb ice stream and the entire Greenland (Figures 11a, 11b, 11d and 11h), the stochastic filter solution and the mascon solution are very consistent in the estimated secular variations. Since no prior information on the Alaska glacier changes has been given at all, the consistency between the secular trends estimated by the stochastic filter and the mascon solution over Gulf of Alaska further supports the previous conclusion that the stochastic filter does not require a very accurate prior mass variation model.

The purpose of this study is to rigorously examine the performance of this novel technique in destriping, rather than presenting any geophysical results with regard to GRACE-estimated mass variations. To do this will require additional considerations such as GIA and leakage corrections.

5. Discussion and Conclusions

We developed a stochastic filter for statistically rigorous separation of geophysical signals and correlated “stripe” noises in a series of GRACE monthly SHC estimates. A major benefit of the technique is that, in stochastically modeling the signals and stripe noises, we are able to realize the destriping in a Bayesian framework, and thus propagate statistically rigorous posterior covariance matrices which reflect the correlated noise and the impact on the SHC uncertainties of the destriping. Gaussian smoothing is not required as the Bayesian approach yields a natural resolution for the geophysical signal that reflects the statistical information on the correlated noise. In using the estimates for studies, further constraints may be applied depending on the application.

Applied to decade-long GRACE RL05 monthly gravity fields, the stochastic filter yields monthly surface mass estimates comparable with the GRACE Tellus solutions in terms of spatial resolution and signal amplitude, wherein the latter are processed using the SW destriping procedure followed by further spatial Gaussian smoothing. One explanation for the differences between our result and the GRACE Tellus solution, especially over the oceans and polar regions, would be the Gaussian smoothing and spherical harmonic truncation applied to the GRACE Tellus solution. Over oceans, the Gaussian filter of larger smoothing radius (500 km half-wavelength compared to 300 km over land) and the truncation to degree 40 greatly reduce the small-scale features; while over polar regions, the radius of 300 km of the Gaussian smoothing is likely too large to preserve the intrinsic GRACE resolution in the areas.

At basin scales, the stochastic filter and the GRACE Tellus solution estimate fairly consistent average mass variations over major river basins. Over the basins where the mass variations are dominated by seasonal components, the discrepancies between the two solutions are well confined within the tight uncertainty ranges rigorously estimated by the stochastic filter, validating the estimated uncertainties and thus the error models of the stochastic filter. Over the areas undergoing continuous mass variations, such as the Alaska glacier and the drainage basins over Antarctica, the GRACE Tellus solution probably underestimates the magnitudes of inter-annual changes, because the stochastic filter always estimates greater secular magnitudes, which are comparable with those from the mascon solution.

The evolving state of the GRACE flight segment, including the ground track repetition, satellite thermal control, star camera outage and data rate, leads to varying errors in each monthly field over time [Bettadpur and the CSR Level-2 Team, 2012]. The decay of the solution quality will be more obvious as GRACE continues to operate at the end of its mission period. Instead of the invariant stochastic model in this study designed to reflect monthly GRACE correlated errors for all months, time-varying month-by-month stochastic models based on GRACE data quality information might further improve the stochastic analysis.

There remains some common features in the stochastic filter estimates that do not seem to be actual signals, such as the east-west remanent stripes. There could be an additional constraint to be included under the fairly realistic assumption that the gravity signals themselves are correlated spatially. To include constraints for spatial correlations, we can conveniently adapt the stochastic filter to work in the spatial domain rather than in the spectral domain as in this study, meaning that we could use the GRACE SH solutions to calculate the mass variation for a global grid (e.g. mascons), and design a more realistic covariance matrix reflecting proper correlations among adjacent grid points. In this way, we would be able to take into account the specific characteristics of spatial correlations associated with different regions, e.g., larger spatial correlation distance (same effect as longer Gaussian smoothing radius) for the estimation of ocean bottom pressure over oceans [Chambers and Bonin, 2012], and smaller correlation distance for the estimation of Antarctic ice mass balance [Jacob *et al.*, 2012]. Also, we would be able to mitigate the leakage of land signals into the ocean by implementing zero correlation across the land-ocean boundary.

A distinct benefit of the stochastic filter technique is that it enables statistically rigorous estimation of the GRACE SHC uncertainty after destriping. Hill *et al.* [2010] developed a Bayesian method for combining multiple data types (GRACE, GPS, tide gauge and GIA models) to estimate GIA rate fields (namely relative sea-level change, gravity, and crustal deformation) and their associated uncertainties. The previous study [Hill *et al.*, 2010] did not deal with GRACE observation in a Bayesian manner, since the GRACE SHCs were destriped based on the SW procedure which includes Gaussian smoothing, and empirical uncertainty is ascribed to the GRACE field after destriping. The stochastic filter developed in our current study, performing the destriping process in the Bayesian context and yielding covariances of the destriped fields, demonstrates that the Bayesian method

works well even in the presence of correlated stripe noise. It would therefore be an appropriate “front-end” for the more statistically rigorous and self-consistent modeling of seasonal and longer-term signals [Davis *et al.*, 2012], and statistical techniques recently developed to combine GRACE and other data for simultaneous estimation of GIA and present-day melting signals [Hill *et al.*, 2010].

Acknowledgments

This research was supported in part by NASANNX11AC14G and NNX14AP33G, the Earth Observatory of Singapore, and the National Oceanographic Centre (UK). E.M.H. was supported by the Earth Observatory of Singapore and by the National Research Foundation Singapore under its Singapore NRF Fellowship scheme (National Research Fellow Award No. NRF-NRFF2010-064). M.E.T. was supported through core funding provided by the National Environment Research Council to the National Oceanography Centre. The GRACE Tellus solution can be downloaded from <http://grace.jpl.nasa.gov/data/gracemonthlymassgridsoverview/>. The CSR RL05 GRACE Level-2 data products can be downloaded from <http://www.csr.utexas.edu/grace/RL05.html>. GRACE Level-2 formal covariance matrices were kindly made available by J. Ries and S. Bettadpur of CSR. Generic Mapping Tools (GMT) [Wessel *et al.*, 2013] were used to make some of the figures in this paper. We thank three anonymous reviewers for their valuable reviews, and Associate Editor Benjamin Chao and Editor Paul Tregoning for their comments and suggestion.

References

- Bettadpur, S., and the CSR Level-2 Team (2012), Assessment of GRACE mission performance and the RL05 gravity fields, Abstract G31C-02 presented at 2012 Fall Meeting, AGU, San Francisco, Calif., 3–7 Dec.
- Boening, C., T. Lee, and V. Zlotnicki (2011), A record-high ocean bottom pressure in the South Pacific observed by GRACE, *Geophys. Res. Lett.*, **38**, L04602, doi:10.1029/2010GL046013.
- Chambers, D. P. (2006), Evaluation of new GRACE time-variable gravity data over the ocean, *Geophys. Res. Lett.*, **33**, L17603, doi:10.1029/2006GL027296.
- Chambers, D. P., and J. A. Bonin (2012), Evaluation of Release-05 GRACE time-variable gravity coefficients over the ocean, *Ocean Sci.*, **8**(5), 859–868, doi:10.5194/os-8-859-2012.
- Chambers, D. P., and J. Schröter (2011), Measuring ocean mass variability from satellite gravimetry, *J. Geodyn.*, **52**(5), 333–343, doi:10.1016/j.jjog.2011.04.004.
- Chen, J. L., C. R. Wilson, B. D. Tapley, and S. Grand (2007), GRACE detects coseismic and postseismic deformation from the Sumatra-Andaman earthquake, *Geophys. Res. Lett.*, **34**, L13302, doi:10.1029/2007GL030356.
- Chen, J. L., C. R. Wilson, and B. D. Tapley (2010), The 2009 exceptional Amazon flood and interannual terrestrial water storage change observed by GRACE, *Water Resour. Res.*, **46**, W12526, doi:10.1029/2010WR009383.
- Davis, J. L., M. E. Tamisiea, P. Elósegui, J. X. Mitrovica, and E. M. Hill (2008), A statistical filtering approach for Gravity Recovery and Climate Experiment, (GRACE) gravity data, *J. Geophys. Res.*, **113**, B04410, doi:10.1029/2007JB005043.
- Davis, J. L., B. P. Wernicke, and M. E. Tamisiea (2012), On seasonal signals in geodetic time series, *J. Geophys. Res.*, **117**, B01403, doi:10.1029/2011JB008690.
- Duan, X., J. Guo, C. Shum, and W. van der Wal (2009), On the postprocessing removal of correlated errors in GRACE temporal gravity field solutions, *J. Geod.*, **83**(11), 1095–1106, doi:10.1007/s00190-009-0327-0.
- Geruo, A., J. Wahr, and S. Zhong (2013), Computations of the viscoelastic response of a 3-D compressible earth to surface loading: An application to glacial isostatic adjustment in antarctica and canada, *Geophys. J. Int.*, **192**(2), 557–572, doi:10.1093/gji/ggs030.
- Han, S.-C., C. K. Shum, C. Jekeli, C.-Y. Kuo, C. Wilson, and K.-W. Seo (2005), Non-isotropic filtering of GRACE temporal gravity for geophysical signal enhancement, *Geophys. J. Int.*, **163**(1), 18–25, doi:10.1111/j.1365-246X.2005.02756.x.
- Han, S.-C., C. K. Shum, M. Bevis, C. Ji, and C.-Y. Kuo (2006), Crustal dilatation observed by GRACE after the 2004 Sumatra-Andaman earthquake, *Science*, **313**(5787), 658–662, doi:10.1126/science.1128661.
- Harig, C., and F. J. Simons (2015), Accelerated west antarctic ice mass loss continues to outpace east antarctic gains, *Earth Planet. Sci. Lett.*, **415**, 134–141, doi:10.1016/j.epsl.2015.01.029.
- Heki, K., and K. Matsuo (2010), Coseismic gravity changes of the 2010 earthquake in central Chile from satellite gravimetry, *Geophys. Res. Lett.*, **37**, L24306, doi:10.1029/2010GL045335.
- Hill, E. M., J. L. Davis, M. E. Tamisiea, and M. Lidberg (2010), Combination of geodetic observations and models for glacial isostatic adjustment fields in Fennoscandia, *J. Geophys. Res.*, **115**, B0740, doi:10.1029/2009JB006967.
- Hill, E. M., J. L. Davis, M. E. Tamisiea, R. M. Ponte, and N. T. Vinogradova (2011), Using a spatially realistic load model to assess impacts of Alaskan glacier ice loss on sea level, *J. Geophys. Res.*, **116**, B10407, doi:10.1029/2011JB008339.
- Jacob, T., J. Wahr, W. T. Pfeffer, and S. Swenson (2012), Recent contributions of glaciers and ice caps to sea level rise, *Nature*, **482**(7386), 514–518.
- Jekeli, C. (1981), Alternative methods to smooth the Earth's gravity field, *Tech. Rep.* 327, Geod. Sci. and Surv. Ohio state Univ., Columbus, Ohio.
- Kim, S.-B., T. Lee, and I. Fukumori (2007), Mechanisms controlling the Interannual variation of mixed layer temperature averaged over the Niño-3 region, *J. Clim.*, **20**(15), 3822–3843, doi:10.1175/JCLI4206.1.
- Kurtenbach, E., T. Mayer-Gürr, and A. Eicker (2009), Deriving daily snapshots of the Earth's gravity field from grace l1b data using kalman filtering, *Geophys. Res. Lett.*, **36**, L17102, doi:10.1029/2009GL039564.
- Kusche, J. (2007), Approximate decorrelation and non-isotropic smoothing of time-variable GRACE-type gravity field models, *J. Geod.*, **81**(11), 733–749, doi:10.1007/s00190-007-0143-3.
- Landerer, F. W., and S. C. Swenson (2012), Accuracy of scaled grace terrestrial water storage estimates, *Water Resour. Res.*, **48**, W04531, doi:10.1029/2011WR011453.
- Luthcke, S. B., T. Sabaka, B. Loomis, A. A. Arendt, J. J. McCarthy, and J. Camp (2013), Antarctica, greenland and gulf of alaska land-ice evolution from an iterated grace global mascon solution, *J. Glaciol.*, **59**, 613–631, doi:10.3189/2013JoG12J147.
- Paulson, A., S. Zhong, and J. Wahr (2007), Inference of mantle viscosity from grace and relative sea level data, *Geophys. J. Int.*, **171**(2), 497–508, doi:10.1111/j.1365-246X.2007.03556.x.
- Pellinen, L. (1970), Estimation and application of degree variances of gravity, *Stud. Geophys. Geod.*, **14**(2), 168–173, doi:10.1007/BF02585615.
- Rapp, R. H. (1973), Improved models for potential coefficients and anomaly degree variances, *J. Geophys. Res.*, **78**(17), 3497–3500, doi:10.1029/JB078i017p03497.
- Ravishanker, N., and D. K. Dey (2002), *A First Course in Linear Model Theory*, Chapman and Hall/CRC, Boca Raton, Fla.
- Rodell, M., et al. (2004), The Global Land Data Assimilation System, *Bull. Am. Meteorol. Soc.*, **85**(3), 381–394, doi:10.1175/BAMS-85-3-381.
- Rowlands, D. D., S. B. Luthcke, J. J. McCarthy, S. M. Klosko, D. S. Chinn, F. G. Lemoine, J.-P. Boy, and T. J. Sabaka (2010), Global mass flux solutions from GRACE: A comparison of parameter estimation strategies-Mass concentrations versus stokes coefficients, *J. Geophys. Res.*, **115**, B01403, doi:10.1029/2009JB006546.
- Sabaka, T. J., D. D. Rowlands, S. B. Luthcke, and J.-P. Boy (2010), Improving global mass flux solutions from Gravity Recovery And Climate Experiment, (GRACE) through forward modeling and continuous time correlation, *J. Geophys. Res.*, **115**, B11403, doi:10.1029/2010JB007533.
- Schrama, E. J. O., B. Wouters, and D. A. Lavallée (2007), Signal and noise in Gravity Recovery And Climate Experiment, (GRACE) observed surface mass variations, *J. Geophys. Res.*, **112**, B08407, doi:10.1029/2006JB004882.
- Shepherd, A., et al. (2012), A reconciled estimate of ice-sheet mass balance, *Science*, **338**(6111), 1183–1189, doi:10.1126/science.1228102.

- Swenson, S., and J. Wahr (2006), Post-processing removal of correlated errors in GRACE data, *Geophys. Res. Lett.*, *33*, L08402, doi:10.1029/2005GL025285.
- Swenson, S. C., and J. M. Wahr (2011), Estimating signal loss in regularized grace gravity field solutions, *Geophys. J. Int.*, *185*(2), 693–702, doi:10.1111/j.1365-246X.2011.04977.x.
- Tamisiea, M. E., J. X. Mitrovica, and J. L. Davis (2007), GRACE gravity data constrain ancient ice geometries and continental dynamics over Laurentia, *Science*, *316*(5826), 881–883, doi:10.1126/science.1137157.
- Tapley, B., et al. (2005), GGM02—An improved Earth gravity field model from GRACE, *J. Geod.*, *79*(8), 467–478, doi:10.1007/s00190-005-0480-z.
- Tapley, B. D., S. Bettadpur, J. C. Ries, P. F. Thompson, and M. M. Watkins (2004), GRACE Measurements of Mass Variability in the Earth System, *Science*, *305*(5683), 503–505, doi:10.1126/science.1099192.
- Wahr, J., M. Molenaar, and F. Bryan (1998), Time variability of the Earth's gravity field: Hydrological and oceanic effects and their possible detection using GRACE, *J. Geophys. Res.*, *103*(B12), 30,205–30,229, doi:10.1029/98JB02844.
- Wahr, J., S. Swenson, and I. Velicogna (2006), Accuracy of grace mass estimates, *Geophys. Res. Lett.*, *33*, L06401, doi:10.1029/2005GL025305.
- Wang, H., L. Jia, H. Steffen, P. Wu, L. Jiang, H. Hsu, L. Xiang, Z. Wang, and B. Hu (2013), Increased water storage in North America and Scandinavia from GRACE gravity data, *Nat. Geosci.*, *6*(1), 38–42.
- Wang, L., C. K. Shum, F. J. Simons, B. Tapley, and C. Dai (2012a), Coseismic and postseismic deformation of the 2011 Tohoku-Oki earthquake constrained by GRACE gravimetry, *Geophys. Res. Lett.*, *39*, L07301, doi:10.1029/2012GL051104.
- Wang, L., C. K. Shum, F. J. Simons, A. Tassara, K. Erkan, C. Jekeli, C. Kuo, H. Lee, and D. N. Yuan (2012b), Coseismic slip of the 2010 Mw 8.8 Great Maule, Chile, earthquake quantified by the inversion of GRACE observations, *Earth Planet. Sci. Lett.*, *335–336*, 167–179, doi:10.1016/j.epsl.2012.04.044.
- Wang, L., C. K. Shum, and C. Jekeli (2012c), Gravitational gradient changes following the 2004 December 26 Sumatra-Andaman Earthquake inferred from GRACE, *Geophys. J. Int.*, *191*(3), 1109–1118, doi:10.1111/j.1365-246X.2012.05674.x.
- Watkins, M. M., D. N. Wiese, D.-N. Yuan, C. Boening, and F. W. Landerer (2015), Improved methods for observing Earth's time variable mass distribution with grace using spherical cap mascons, *J. Geophys. Res.*, *120*(4), 2648–2671, doi:10.1002/2014JB011547.
- Wessel, P., W. H. F. Smith, R. Scharroo, J. Luis, and F. Wobbe (2013), Generic mapping tools: Improved version released, *Eos Trans. AGU*, *94*(45), 409–410, doi:10.1002/2013EO450001.
- Williams, S. D. P. (2003), The effect of coloured noise on the uncertainties of rates estimated from geodetic time series, *J. Geod.*, *76*(9–10), 483–494, doi:10.1007/s00190-002-0283-4.
- Zhang, Z.-Z., B. F. Chao, Y. Lu, and H.-T. Hsu (2009), An effective filtering for grace time-variable gravity: Fan filter, *Geophys. Res. Lett.*, *36*, L17311, doi:10.1029/2009GL039459.